HHS Public Access

Author manuscript

Sci Transl Med. Author manuscript; available in PMC 2018 May 22.

Published in final edited form as:

Sci Transl Med. 2017 November 22; 9(417): . doi:10.1126/scitranslmed.aan8462.

Large-scale proteomics identifies MMP-7 as a sentinel of epithelial injury and of biliary atresia

Chatmanee Lertudomphonwanit[1,4], **Reena Mourya**[1], **Lin Fei**[2], **Yue Zhang**[2,†], **Sridevi Gutta**[1], **Li Yang**[1,5], **Kevin E. Bove**[3], **Pranavkumar Shivakumar**[1], and **Jorge A. Bezerra**[1,*]

[1]Division of Gastroenterology, Hepatology and Nutrition and the Department of Pediatrics of the University of Cincinnati College of Medicine, Cincinnati, OH, USA [2]Division of Biostatistics and Epidemiology and the Department of Pediatrics of the University of Cincinnati College of Medicine, Cincinnati, OH, USA [3]Division of Pathology of Cincinnati Children's Hospital Medical Center and the Department of Pediatrics of the University of Cincinnati College of Medicine, Cincinnati, OH, USA [4]Division of Gastroenterology and Hepatology, Department of Pediatrics, Ramathibodi Hospital, Mahidol University, Bangkok, Thailand [5]Division of Pediatric Surgery, Union Hospital, Tongji Medical College, Huazhong University of Science and Technology, Wuhan, China

Abstract

Biliary atresia is a progressive infantile cholangiopathy of complex pathogenesis. Although early diagnosis and surgery are the best predictors of treatment response, current diagnostic approaches are imprecise and time consuming. We used large-scale, quantitative serum proteomics at the time of diagnosis of biliary atresia and other cholestatic syndromes (serving as disease controls) to identify biomarkers of disease. In a discovery cohort of 70 subjects, the lead biomarker was matrix metalloproteinase-7 (MMP-7), which retained high distinguishing features for biliary atresia in two validation cohorts. Notably, the diagnostic performance reached 95% when MMP-7 was combined with gamma-glutamyltranspeptidase (GGT), a marker of cholestasis. Using human tissue and experimental model of biliary atresia, we found that MMP-7 is primarily expressed by cholangiocytes, is released upon epithelial injury, and promotes the experimental disease phenotype. Thus, we propose that serum MMP-7 (alone or in combination with GGT) is a diagnostic biomarker for biliary atresia and may serve as a therapeutic target.

*Corresponding author. jorge.bezerra@cchmc.org (J.A.B.).

†Current address: Department of Bioinformatics and Biostatistics, School of Life Sciences and Biotechnology, Shanghai Jiao Tong University, Shanghai, China.

Author contributions

JAB, PS, and CL designed the research work. PS, CL, LY, and SG performed the animal experiments. JAB, PS, CL, RM and KEB analyzed data. LF, YZ, and CL performed statistical analyses. CL and JAB wrote and edited the manuscript. All contributing authors assisted in reviewing the manuscript.

Competing Interests

The authors declare no competing interests.

Data and materials availability

Data on protein expression are submitted as a Supplementary Material.

Introduction

Diagnostic accuracy and timeliness are critical for therapeutic interventions that target pathogenesis of diseases. When diseases are caused by well-defined sequence variants in gene or gene groups, the use of mutation screening tests simplifies diagnostic algorithms and allows for the personalization of treatments (1, 2). Unfortunately, the opportunities for molecular diagnosis or targeted treatments are limited in diseases of multifactorial etiology and complex pathogenesis (3, 4). Biliary atresia (BA) is such a disease prototype, with increasing evidence for viruses, environmental toxins, and susceptibility genes as etiologic agents, and a dysregulated immune response that disrupts the epithelial lining and limits tissue repair (5–8). This rare disease results from a rapidly progressive inflammatory and fibrosing injury to extrahepatic bile ducts that interrupts the flow of bile and produces severe liver injury in otherwise healthy infants. With an onset of pathological jaundice limited to a highly reproducible window in the first 3–4 months of life of affected infants, the early diagnosis and surgical intervention are critical for the restoration of bile flow and improvement in short-term outcome (7, 9, 10). However, neonatal jaundice is a common sign for several clinical syndromes. Clinical algorithms have been proposed to differentiate BA from other causes of neonatal cholestasis (7, 11, 12), but they are imprecise and have the potential to delay the diagnosis and treatment (12).

Previous studies analyzing the serum and plasma by metabolomics, enzyme-linked immunosorbent assays and microRNA quantification have yielded potential biomarkers of BA (13–15). However, the use of small cohorts and the lack of prospective validation in these studies limit the application of the findings in diagnosis or screening. Efforts to investigate whether the concentration of circulating cytokines linked to pathogenesis of the biliary injury such as IL-2, IL-10, TNF-α, and IL-8 fall short of reliably differentiating BA from other cholestatic syndromes (16, 17). Here, we report the proteomic analysis of serum samples at the time of diagnosis of BA, which uncovered high circulating levels of matrix metalloproteinase-7 (MMP-7) above the levels of age-matched disease and healthy controls. After demonstrating the reproducibility of the findings in two validation cohorts, we explored its potential role in the pathogenesis of tissue injury. We found that the MMP-7 is constitutively expressed by normal cholangiocytes, increases in the serum upon biliary injury, and modulates the clinical phenotype in an experimental model of BA.

Results

Serum proteomics of biliary atresia in a discovery cohort

To search for biomarkers of BA, we applied the Slow Off-rate Modified Aptamer scan (SOMAscan®, Somalogic Inc., Boulder, CO, USA) to 70 serum samples from a discovery cohort of infants at the time of diagnosis of BA (at Kasai operation, N=35) and in age-matched infants with neonatal intrahepatic cholestasis (IHC; N=35; Fig. 1), as described previously (18). Infants were enrolled into a prospective study of the NIDDK-funded Childhood Liver Disease Research Network (ChiLDReN; www.childrennetwork.org; Clinicaltrials.gov Identifier: NCT00061828). All groups were age-matched and had similar levels of hepatocellular injury and cholestasis (Table 1), except for a higher level of gamma-glutamyltranspeptidase (GGT) in infants with BA ($P < 0.0001$). Out of 1,129 proteins, 76

were significantly over- or under- expressed in BA compared to IHC (FDR adjusted *P*-value < 0.05; table S1), with the top 9 differentially expressed proteins shown in Figure 2.

To explore the potential value of these proteins as biomarkers of disease, we used multivariable logistic regression analyses and uncovered that the combination of MMP-7 and ectonucleotide pyrophosphatase/phosphodiesterase family member 7 (ENPP7) distinguished BA from IHC with Area Under the Receiver Operating Characteristic (ROC) curve (AUC) of 0.99 (95% CI: 0.97 to 1.00; Fig. 3A and C). Between the two proteins, MMP-7 alone showed excellent diagnostic features with an AUC of 0.97 (95% CI: 0.93 to 1.00), and a sensitivity of 97% and specificity of 91% at cut-off probability of 0.49. Taking into account the relatively low AUC of 0.78 for ENPP7 and the previous reports that serum GGT is generally higher in infants with BA (19, 20), we next examined how the combination of serum MMP-7 and GGT (available from the biochemical studies; N=29 for BA and 31 for IHC; Fig. 3B) would compare to MMP-7 + ENPP7. Although GGT alone generated an AUC of 0.9 (95% CI: 0.83 to 0.97; Fig. 3B and C), the AUC for MMP-7 + GGT at 0.98 (95% CI: 0.94 to 1.00) was not superior to MMP-7 + ENPP7. Collectively, the data on this discovery cohort were preliminary evidence that the combination of MMP-7 with ENPP7 or GGT had a potentially high diagnostic accuracy for infants with BA.

Validation of MMP-7 as a biomarker of biliary atresia

To test the reproducibility of the high accuracy for MMP-7, ENPP7 and GGT alone or in combination in BA, we performed the same SOMAscan® assay in two other independent cohorts separately (Fig. 1). The first cohort consisted of a similar number of age-matched infants with BA or IHC. To determine the assay reproducibility, we included 6 samples assayed from the discovery cohort to serve as bridging samples, and found a high correlation r = 0.9958 (95% CI: 0.9956 to 0.9960) between the two assays. Using the same analytical approach as in the discovery cohort, the different combinations of the serum biomarker and GGT produced lower AUCs than in the discovery cohort, except for a persistently high AUC of 0.94 for MMP-7 + GGT (95% CI: 0.88 to 1.00; Fig. 4A). In the second validation cohort, we performed a SOMAscan® assay in 105 age-matched infants with BA, and used the MMP-7 abundance signals and the serum GGT values in a discriminatory model for BA. Using the cut-off probability from the discovery cohort to assess the probability of a true positive and a false negative, the MMP-7 + GGT model showed sensitivity of 96% to predict BA (table S2).

Based on the reproducibility of the findings in the validation cohorts, we next examined whether MMP-7 would aid in solving the clinical conundrum of differentiating BA from syndromes of IHC with high serum GGT. For this analysis, we hypothesized that serum MMP-7 maintains high discriminatory features for BA in subjects with serum GGT>300 U/L, a level that has been reported as more frequent in BA (19, 20). For this analysis, we combined all subjects in the discovery and validation cohort #1 (GGT levels available for 122 subjects), which were classified into groups: **(a)** GGT <100 U/L (N=0 for BA, N=24 for IHC), **(b)** GGT=100–300 U/L (N=10 for BA, N=25 for IHC) and **(c)** GGT >300 U/L (N=50 for BA, N=13 for IHC). The analysis for group **(a)** was not pursued because it contained no infant with BA. For groups **(b)** and **(c)**, the AUCs for MMP-7 (0.92 and 0.88, respectively)

and MMP-7+GGT (0.93 and 0.88, respectively) were higher than GGT (0.63 and 0.73, respectively) (Fig S1).

Examining the potential use of serum MMP-7 to diagnose infants with BA, we calculated the "number needed to misdiagnose" (NNM) as a means to estimate the number of patients assigned the correct diagnosis of BA before a misdiagnosis occurs (21). The NNM for MMP-7 was 13.4 (meaning that 1 out of 13.4 patients is misdiagnosed), which was superior to the NNM of 5.4 for GGT (1 out of 5.4 is misdiagnosed). Notably, the combination of MMP-7 + GGT had the best NNM at 19.1. Overall, this estimation emphasized the benefit of serum MMP-7 (alone or in combination) over GGT as a diagnostic aid for BA.

Validation by an antibody-based assay

To determine whether the high levels of MMP-7 could be validated using a different technology, we obtained serum aliquots from 10 infants in the discovery cohort and determined the MMP-7 concentration using an antibody-based enzyme-linked immunosorbent assay. The direct measurement of MMP-7 was high for BA and had no overlap with IHC (Fig. 4B). Interestingly, a comparative plot using SOMAscan® data for the same subjects showed a greater separation between the cohorts (Fig. 4C). Taken together, these data confirmed the performance of MMP-7 + GGT as having a high accuracy for the diagnosis of BA, with validation in two independent cohorts and technical reproducibility using an antibody-based assay.

Expression of MMP-7 in extrahepatic ducts and cholestatic syndromes

Searching for the biological basis of the increased serum levels of MMP-7 in BA, we first stained paraffin-embedded sections of human liver (normal segment from liver tumor resection), gallbladder (normal histology after cholecystectomy of adult subject) and extrahepatic bile ducts (EHBD, from a stillborn neonate). We focused on these tissues because of the predominant expression of MMP-7 in the liver and biliary system reported in the Human Protein Atlas (http://www.proteinatlas.org/ENSG00000137673-MMP7/tissue). Our immunostaining showed minimal or no expression of MMP-7 in parenchymal or non-parenchymal cells of the normal liver. In contrast, the protein was uniquely expressed in the cytoplasm of cholangiocytes along the epithelium of the gallbladder, EHBD, and surrounding peribiliary glands (Fig. 5A).

In liver biopsies obtained at the time of diagnosis of BA, MMP-7 was detected in cholangiocytes of intrahepatic bile ducts in most samples, albeit at variable levels, and in few hematopoietic cells within the portal tracts (N=12; Fig. 5B and D). Interestingly, a lighter expression pattern was detected in liver biopsies of infants with alpha-1-antitrypsin deficiency (N=6; Fig. 5C and D) and idiopathic neonatal cholestasis (N=2), which may account for the increased serum level in IHC above healthy controls. To determine MMP-7 expression at the transcriptional level, we extracted liver mRNA data from the genome-wide expression datasets for subjects with BA (N=64), IHC (N=14) and normal controls (N=7) which we published previously and submitted to the Gene Expression Omnibus (GSE46995) (17). Consistent with histological findings, livers from BA subjects had higher *MMP-7* mRNA expression compared to IHC (fold change to normal controls = 9.98 ± 7.65 versus

2.54 ± 1.73; P < 0.0001; Fig. 4D). Interestingly, the mRNA expression for *GGT* in these biopsies was not significantly different between the groups, revealing a discrepancy at the hepatic transcriptional level when compared to the differences in serum GGT (Fig S3A). Together, these data defined a primary localization of MMP-7 in cholangiocytes of EHBDs, with a lower level in intrahepatic cholangiocytes in diseased livers. At the whole tissue level, the total liver *MMP-7* mRNA was still higher in BA when compared to diseased controls.

Lack of correlation between MMP-7 and fibrosis

To explore the biological properties of MMP-7 in determining the phenotype of extrahepatic cholangiopathies, we first investigated the relationship between MMP-7 expression and tissue fibrosis. Based on the well-described role of metalloproteinases in the turnover and degradation of extracellular matrix and on the previous reports linking MMP-7 to elastin, e-cadherin, and syndecan-1 (22–24), we hypothesized that MMP-7 expression correlated with the severity of liver fibrosis. To test this hypothesis, we analyzed the relationship between serum MMP-7 and histological fibrosis using the Scheuer fibrosis staging 0–4, as described previously (25). For these experiments, the fibrosis staging was performed independently by the pathologists of the ChiLDReN consortium in liver biopsy samples from the same subjects with BA whose sera were analyzed by the SOMAscan® assay. Serum MMP-7 correlated poorly with liver fibrosis staging at the time of diagnosis (Spearman r = 0.33; 95% CI: 0.17 to 0.48, P < 0.0001; fig. S2A). Similarly, ROC analysis showed that serum MMP-7 was a poor predictor of hepatic fibrosis (AUC = 0.69; 95% CI: 0.59 to 0.78; fig. S2B). To investigate whether the expression of MMP-7 correlated with fibrosis within the same tissue, we compared the surface area of hepatic fibrosis detected by trichrome staining and of the area immunostained by MMP-7 (fig. S2C). Again, MMP-7 expression in the liver had very low correlation with hepatic fibrosis (Spearman r = 0.25; P=0.52; fig. S2D). Collectively, these data did not support a functional role of MMP-7 in modulating the fibrosing phenotype at the time of diagnosis of BA.

Increase of MMP-7 upon experimental biliary injury

Without evidence that MMP-7 is linked to hepatic fibrosis in BA, we next explored whether the protein is involved in the inflammatory mechanisms that regulate epithelial injury. Based on the proposed role of MMP-7 in activating the innate immune response to a tissue injury (26), we first determined whether serum levels of MMP-7 increase in neonatal mice following bile duct epithelial injury induced by rotavirus infection. In this model, the intraperitoneal administration of $1.5x10^6$ fluorescent forming units of rhesus rotavirus type-A (RRV) into BALB/c mice within 24 hours of birth injures the epithelial lining of EHBD, followed by an inflammatory obstruction of the lumen and atresia (27, 28). As expected, RRV infection resulted in obstruction of EHBD, jaundice, growth retardation and acholic stools; universal mortality occurred by day 15 of viral challenge (29). Analyzing serum samples collected 7 days after RRV injection (time of the peak of epithelial injury), the concentration of MMP-7 increased significantly above the levels of age-matched, saline-injected controls (2.01 ± 0.39 versus 0.96 ± 0.14 ng/mL; N=3–4 per group; P = 0.03; Fig. 6A). In the liver, RT-PCR revealed *Mmp-7* expression significantly increased at 14 days after RRV injection (P < 0.0001; Fig. 6B) while in EHBD *Mmp-7* increased by 20 and 6 fold higher at 7 and 14 days, respectively, after RRV injection (P < 0.0001; Fig. 6C). This pattern

of mRNA expression differed from *Ggt1*, which only increased in the liver 3 days after RRV (Fig. S3B and C).

To examine whether the cellular source of Mmp-7 expression in neonatal mice was similar to the pattern in humans, we immunostained livers and EHBD at days 3, 7, and 14 days of life of saline-injected mice (serving as controls) and after RRV injection. In control mice, the hepatic expression of Mmp-7 was detected in extramedulary hematopoietic cells and restricted to the first 3 days of life, while the pattern in EHBDs was predominantly localized to cholangiocytes lining the entire length of the duct epithelium, cholangiocytes of neighboring peribiliary glands, and in few subepithelial cells at all time points (Fig. 6D and E). Following RRV infection, Mmp-7 was detected in inflammatory cells infiltrating the periductal space of portal tracts at 7 and 14 days (Fig. 6D), with a broader staining pattern in epithelial cells and subepithelial compartment of EHBD (Fig. 6E). Altogether, the immunostaining pattern revealed a striking similarity with findings in human tissues, in which Mmp-7 is expressed predominantly by cholangiocytes of EHBDs, with a release to the serum triggered by the epithelial injury. These findings raised the possibility that Mmp-7 may be involved in the regulation of the phenotype of experimental BA.

Suppression of experimental biliary atresia by Batimastat and MMP-7 antibody

To directly test whether Mmp-7 plays a mechanistic role in pathogenesis of biliary injury, we injected the matrix metalloproteinase inhibitors Batimastat (with activity against MMP-7) or GM6001 (without activity against MMP-7) intraperitoneally on days 1, 3, 5, and 7 after RRV injection; the vehicle (5% DMSO, 28.5% propylene glycol, 5% Tween 80, and 62% of 0.9% NaCl) was injected into a separate group of RRV-infected mice serving as controls. First, we evaluated whether other matrix metalloproteinases were upregulated in the experimental model at the time of bile duct obstruction and onset of symptoms (7 days after RRV challenge). We found minimal or no change in the mRNA expression of *Mmp-2, Mmp-3, Mmp-8, Mmp-9, Mmp-10, Mmp-12, Mmp-13* and *Mmp-14* in the liver and EHBD, with only *Mmp-7* increasing in the liver by 2 fold and in EHBD by 89 fold above controls (Fig. 7A). Those RRV-infected experimental and control mice injected with Batimastat, GM6001 or vehicle were sacrificed at 12–14 days for tissue analyses. In the liver, the histological features of portal inflammation and hepatocellular necrosis were mild in Batimastat-treated mice, and moderate or severe in mice treated with vehicle or GM6001 (Fig. 7B and D). The beneficial effects of Batimastat were even more pronounced in EHBDs, where it prevented epithelial injury and duct obstruction in 86% of neonatal mice, while all EHBDs were obstructed in mice injected with GM6001 or vehicle (Fig. 7C and D). Consistent with these histological findings, the use of Batimastat resulted in the selective suppression of mRNA expression for *Tnfa, Cxcl9,* and the three murine orthologs of *IL8* (*Cxcl1, Cxcl2,* and *Cxcl5*) 14 days after RRV infection, which have been shown previously to be increased in livers of children with BA and effectors of biliary injury in mice (29), without changes in the expression of *Cxcl10, Cxcl11*, *Ifng,* or *IL12p40* (Fig. 7E).

To more rigorously examine the impact of inhibition of MMP-7 in the development of the obstructive phenotype in experimental BA, we injected neutralizing anti-MMP-7 antibodies (AF-907, Biotechne, Minneapolis, MN, USA) intraperitoneally daily to 12 newborn mice at

days 1–5 after RRV inoculation; control mice received goat serum. All mice were sacrificed 12 days later. Histologically, the liver injury varied from mild to moderate, with a notable prevention of the duct obstruction as shown by patency of EHBDs in 82% of the mice, similarly to the phenotype observed followed administration of Batimastat (Fig 7B–D), while all control mice receiving goat serum had the full obstructive phenotype of EHBDs.

Discussion

Applying large-scale quantitative proteomics to sera of infants with BA, we found high circulating levels of soluble proteins at the time of diagnosis of BA. Chief among them was MMP-7, whose expression distinguished the disease from other causes of intrahepatic cholestasis. The prospective validation of these findings in two independent cohorts pointed to the value of MMP-7 as a biomarker of BA, with an even greater discriminatory value when linked to the serum levels of GGT. Searching for the biological basis of high circulating MMP-7, *in situ* immunostaining localized MMP-7 expression in cholangiocytes along the epithelium of extrahepatic bile ducts and gallbladder of normal subjects, and to a lower extent in intrahepatic cholangiocytes of diseased livers. A similar expression pattern was present in neonatal mice, in whom modeling of the disease demonstrated a release of Mmp-7 into the circulation upon epithelial injury. Notably, the pharmacologic inhibition by Batimastat and the antibody neutralization of MMP-7 suppressed the experimental BA phenotype, with lower expression of *Tnfa, Cxcl9,* and the three murine orthologs of *IL8* related signals and decreased tissue injury. Altogether, these findings support a role for serum MMP-7 levels as a biomarker of BA, and a unique cellular expression in the extrahepatic epithelium that suggested a direct implication in pathogenesis of disease.

The discovery of minimally invasive biomarkers highly predictive of BA is crucial for the timely diagnosis and stratification of care. Despite the well-recognized value of young age as a key factor associated with the best surgical outcome, the overlapping clinical and biochemical features shared between BA and other causes of neonatal cholestasis create a formidable diagnostic challenge that leads to a delay in surgery. Here, the finding that the quantification of a single protein biomarker with an accuracy of 94.3% for BA has the potential to greatly simplify diagnostic approaches, especially when the findings are validated in two separate cohorts and by a different assay/technology. Interestingly, our data point to a potential advantage of the aptamer-based quantification by its seemingly greater separation of the two different disease groups when compared to the results of an antibody-based assay; such superiority, however, requires additional validation.

Among the published biomarkers of BA, serum GGT levels have the highest sensitivity and specificity of 40% and 98%, respectively (19), which may reach up to 83% and 82% in infants age 61–90 days (20). The analysis of the behavior of GGT in our cohorts showed higher levels in BA, with 83% sensitivity and 81% specificity to predict the disease. Interestingly, when we coupled serum MMP-7 with GGT in a composite model we obtained higher sensitivity and specificity of 97% and 94%, at optimal cut-off, which provided positive and negative predictive values of 85% and 99% if one considers the prevalence of BA of 25.9% among infants with conjugated hyperbilirubinemia (30). Other candidate biomarkers previously reported include miR-140-3p (31), miR-200b/429 (14), miR-4429,

and miR-4689 (32), but with lower sensitivity (66–83%) and specificity (79–83%) and no prospective validation. In a separate study, the use of 2-dimensional gel electrophoresis with tandem mass spectrometry found a combination of 11 proteins as biomarkers; the small cohort size and relatively large number of protein analytes selected in this study limit the interpretation of the results and its potential use in clinical practice (33). Altogether, these data suggest a superior value for MMP-7 + GGT among circulating biomarkers of BA. Their predictive features may extend beyond the published predictive value of liver histology in BA (25, 34). In fact, assuming the existence of some degree of variability among pathologists to accurately interpret histological features in the liver that are diagnostic of extrahepatic obstruction (25), the non-invasive, non-operator dependent features suggest that the measurement of serum MMP-7 + GGT early in diagnostic algorithms may substantially facilitate the evaluation of cholestatic infants and establish the diagnosis of BA.

The singular emergence of MMP-7 from a comprehensive proteomic analysis points to a potential link to pathogenic mechanism(s) of disease. Previous studies have reported MMP-7 as a diagnostic or prognostic marker for various malignancies, including cholangiocarcinoma, pancreatic carcinoma, and gastric cancer, as well as fibrosis of lung and liver (35–39). Of specific relevance to our findings, MMP-7 was previously reported as elevated in serum and liver samples from subjects with BA after surgical treatment (40, 41), correlating with the severity of fibrosis regardless of the degree of jaundice clearance (41). Testing this possibility, however, we found no or weak correlation between the expression of MMP-7 in the serum or in the liver with the degree of hepatic fibrosis at the time of diagnosis. It remains possible that the levels of serum MMP-7 may change following surgical treatment and be a useful marker of progression of tissue fibrosis.

The close relationship between MMP-7 and BA raises a potential role for MMP-7 in pathogenesis of disease. Its predominant expression in normal extrahepatic cholangiocytes and the variable detection in intrahepatic ducts of diseased livers (from patients with BA and intrahepatic cholestasis) link its increase in the serum to a response to tissue injury. Making use of the mouse model of experimental BA, we directly demonstrated this possibility by the timely rise of serum Mmp-7 after rotavirus injury of extrahepatic bile ducts. In published reports by other investigators, the release of MMP-7 after injury of the lung epithelium was shown to promote shedding of syndecan-1 and Cxcl-8 and create a pericellular chemokine gradient that controls the influx and activation of neutrophils at the injury site (26). Further, MMP-7 may modulate tissue repair by cleaving E-cadherin and disrupting adherens junctions to facilitates cell migration, and inflammation by activation of Fas ligand and latent TNF-α (26, 42). Therefore, we performed proof-of-principle studies to investigate the role of MMP-7 in pathogenesis of biliary injury by using antibody neutralization or inhibition by Batimastat. Both agents prevented the obstruction of EHBDs in >80% of neonatal mice infected with RRV and decreased the expression of IL-8 orthologs and TNF-α (in mice treated with Batimastat).

We recognize that acquisition and analysis of samples and data in a prospective fashion are important to determine the diagnostic utility of MMP-7. To overcome the intrinsic challenge of designing such a study in a disease of very low incidence like biliary atresia, we used blood samples and clinical data collected prospectively from subjects over several years,

then simulated a prospective study design by randomly assigning the samples into the discovery and validation cohorts prior to any assay or analysis. Next, we performed the SOMAscan® and analyzed the data in the discovery cohort. Only then, we sequentially validated the findings in the two test cohorts, thus strengthening the evidence for MMP-7 as a biomarker of disease. Another limitation is that our study design did not include several sub-cohorts of infants with specific syndromes of neonatal cholestasis. This limitation was largely due to the rare nature of these diseases and to our objective of building a diseased-cohort that will more closely replicate the most common clinical scenario that includes idiopathic neonatal cholestasis (the majority of which has spontaneous recovery) and a few patients with specific syndromes, such as Alagille syndrome and deficiencies of canalicular transporters that are not readily distinguishable clinically. These limitations notwithstanding, we report a unique increase in serum MMP-7 at the time of diagnosis of BA, with levels above age-matched diseased and normal controls, and high predictive features as a biomarker of disease. Combining these findings with the rise of serum MMP-7 after experimental biliary injury and the preliminary evidence that it modulates tissue injury and inflammation, we propose that MMP-7 has role in pathogenesis of disease. Clinically, the implications of our findings relate to the potential incorporation of serum MMP-7 alone or in combination with GGT in diagnostic algorithms in the clinical setting, and to future studies to investigate whether the longitudinal measurement of serum MMP-7 may also be used to monitor progression of liver injury and fibrosis.

Materials and Methods

Human Samples

Serum samples, clinical and histological data were obtained from infants with cholestasis enrolled into the Prospective Database of Infants with Cholestasis (PROBE study; Clinical Trials.gov Identifier: NCT00061828) of the NIDDK-funded Childhood Liver Disease Research Network (ChiLDReN; www.childrennetwork.org). PROBE was designed to acquire longitudinal, prospective clinical and laboratory data in a standardized fashion at defined time points. The diagnosis of BA was confirmed by the finding of luminal obstruction of EHBD by histopathological examination. The correlation of liver fibrosis with serum MMP-7 used histological grade scores generated by ChiLDReN pathologists for liver biopsy samples from the same subjects with BA whose sera were analyzed by the SOMAscan® assay. Sera were collected at the time of diagnosis (initial evaluation prior to or at the time of Kasai portoenterostomy) from 175 BA subjects; 70 other subjects with IHC served as disease controls. The diagnoses of the subjects in IHC included idiopathic neonatal hepatitis (N=1), Alagille syndrome (N=2), progressive familial intrahepatic cholestasis (N=1), cytomegalovirus hepatitis (N=1), neonatal sclerosing cholangitis (N=1), mitochondrial DNA depletion syndrome (N=1), endocrinopathy (N=1) and cholestasis of unknown etiology (N=62). Serum samples were also obtained from 9 subjects at 2–3 years of age (organ donors without history of prior liver disease) to serve as normal controls. Tissue sections for immunostaining were obtained from de-identified paraffin-embedded liver tissues archived in the Biobank Repository of Cincinnati Children’s Hospital Medical Center; the diagnosis followed the same criteria used for subjects enrolled in ChiLDReN. All samples were obtained after informed consent from patients' parents/legal guardians.

The study protocols were approved by the human research review boards of all participating institutions.

Mice

Newborn BALB/c mice were injected with $1.5x10^6$ fluorescent-forming units of RRV or 0.9% NaCl (saline) within 24 hours after birth to induce experimental biliary injury and obstruction according to protocols published previously (29). Mice were monitored daily, and subgroups of mice were sacrificed at days 3, 7, and 14 days for serum and tissue examination. Additional groups of mice were injected intraperitoneally with 30 μg/day of Batimastat (BB-94, ApexBio, Houston, TX, USA) or 3 μg/day of GM6001 (ApexBio) daily at 1, 3, 5, and 7 days after RRV injection; the vehicle (5% DMSO, 28.5% propylene glycol, 5% tween 80, and 62% of 0.9% NaCl) was used in the control group. A separate group of neonatal mice received 10 μg of goat-derived, anti-human MMP-7 antibody (AF-907, Biotechne, Minneapolis, MN, USA) intraperitoneally at days 1–5 after RRV infection; controls included a similar volume of goat serum. Analyses and scoring of tissues are described in Supplementary Methods. The Animal Care and Use Committee at CCHMC approved all experiments involving laboratory animals.

Proteomic assay

Serum samples were subjected to the SOMAscan® protein analysis platform (Somalogic Inc., Boulder, CO, USA). The assay measures 1,129 proteins simultaneously using aptamers-based technology; detailed information on assay protocols and specificity has been described elsewhere (18). To determine the inter-assay reproducibility, we provided the same samples to every run (serving as bridging samples, N=6).

Study design of biomarker discovery and statistical analysis

Without *a priori* data on the serum concentration of 1,129 proteins in the first year of life, we did not estimate a sample size and instead built a discovery cohort with a convenience size of N=35 for BA and for IHC. Then we developed a validation cohort #1 that matched the same numbers for BA and IHC (N=35 for each), and additional samples of BA only as validation cohort #2 (N=105) without inclusion of IHC due to the lack of available samples. All protein results were log transformed to accommodate the wide range of assayed proteins, and skewness of their measurement values. Statistical analyses and graphic presentation were conducted using the SAS software, Version 9.3. First, we chose the candidate proteins using Student T-test with False Discovery Rate correction (Benjamini-Hochberg procedure) in the discovery cohort; significant criteria were adjusted P (Q-value) <0.05 between BA versus IHC. Then, we applied multivariable stepwise logistic regression analysis to the list of candidate proteins to identify proteins that best discriminate BA from IHC. The diagnostic performance of the biomarkers was assessed by analyzing ROC curves and calculating for the area under the curves of each model. The sensitivity (true positive) and the specificity (true negative) were determined at optimal cutoff probability. Positive and negative predictive values were calculated using prevalence of BA among infants with cholestasis reported in the literature (30). Likewise, the ROC analyses were used to validate the diagnostic performance of each model in the validation cohort #1. In the second validation, since the cohort consisted of BA subjects only, we used the cut-off probability

from the discovery cohort to assess the probability of true positive and false negative, followed by calculation of sensitivity. Other statistical analyses included descriptive statistics, analysis of variance, Kruskal-Wallis test, and Spearman and Pearson correlations. Differences were considered statistically significant at $P < 0.05$.

Singleplex Bead-based assay and PCR

MMP-7 concentrations in the sample supernatants were determined by enzyme-linked immunosorbent assay (ELISA) using Milliplex™ Multiplex kits (Millipore, Billerica, MA, USA) according to manufacturer's protocol (as described in Supplementary Methods).

Immunohistochemistry and automated image analysis

Immunohistochemistry was performed on 5 μm paraffin-embedded tissue sections as described previously (43), using 1:50 polyclonal MMP-7 antibody (Cloud-Clone Corp, Houston, TX, USA) in human and mouse tissue. An additional liver biopsy slide from each BA subject was subjected for Masson's trichrome staining. Assay description, digital imaging and image analysis are described in Supplementary Methods.

Microarray analysis

We obtained data on *MMP-7* expression from the genome-wide expression datasets of human liver samples of BA, IHC and healthy controls (as above) reported by us previously and submitted to the Gene Expression Omnibus (data accessible at NCBI GEO database [Bessho et al., 2014], accession GSE46995) (17). The datasets were extracted as Affymetrix CEL files and subjected into the GeneSpring software (Agilent Technologies, Santa Clara, CA, USA) for analyses.

Quantitative PCR

Total RNA was isolated from the livers and EHBDs of RRV- or saline-injected BALB/c mice with or without Batimastat- or vehicle- injection using the RNeasy Mini Kit, according to manufacturer's protocol (Qiagen Inc), as described previously.(29) Real-time PCR was used to quantify mRNA for *Mmp-7, Ggt1, Cxcl1, Cxcl2, Cxcl5, Cxcl9, Cxcl10, Cxcl11*, *Tnfa, Ifng, and IL12p40* (Supplementary Methods; table S3).

Supplementary Material

Refer to Web version on PubMed Central for supplementary material.

Acknowledgments

The studies were supported by the generous support of the Junior Co-Operative Society of Cincinnati Children's Hospital Medical Center. Serum and liver tissues were obtained as an ancillary study of the NIDDK-funded Childhood Liver Disease Research Network (ChiLDReN, DK-62497). The authors thank the Pathologists of ChiLDRen for reviewing and scoring all histological specimens, the Data Coordinating Center for managing all studies and providing data and specimens, and the Principal Investigators and Clinical Research Coordinators of individual ChiLDREN Centers for patient recruitment and acquisition of tissue and data. The contents of the article do not necessarily reflect the opinions or views of the NIDDK, ChiLDREN or ChiLDREN investigators.

Funding

Supported by the NIH grants DK-64008 and DK-83781 to JAB and by the Integrative Morphology and the Gene Analysis Cores of the Digestive Health Center (DK-78392).

Non-standard abbreviations

BA	Biliary atresia
IHC	Intrahepatic cholestasis
MMP-7	Matrix metalloproteinase type 7
ENPP7	Ectonucleotide pyrophosphatase/phosphodiesterase family member 7
NC	Normal control
RRV	Rhesus rotavirus

References

1. Liu C, Aronow BJ, Jegga AG, Wang N, Miethke A, Mourya R, Bezerra JA. Novel resequencing chip customized to diagnose mutations in patients with inherited syndromes of intrahepatic cholestasis. Gastroenterology. 2007; 132:119–126. [PubMed: 17241866]
2. Yang Y, Muzny DM, Reid JG, Bainbridge MN, Willis A, Ward PA, Braxton A, Beuten J, Xia F, Niu Z, Hardison M, Person R, Bekheirnia MR, Leduc MS, Kirby A, Pham P, Scull J, Wang M, Ding Y, Plon SE, Lupski JR, Beaudet AL, Gibbs RA, Eng CM. Clinical whole-exome sequencing for the diagnosis of mendelian disorders. N Engl J Med. 2013; 369:1502–1511. [PubMed: 24088041]
3. Boyapati RK, Kalla R, Satsangi J, Ho GT. Biomarkers in Search of Precision Medicine in IBD. Am J Gastroenterol. 2016; 111:1682–1690. [PubMed: 27670602]
4. Hyman DM, Taylor BS, Baselga J. Implementing Genome-Driven Oncology. Cell. 2017; 168:584–599. [PubMed: 28187282]
5. Bessho K, Bezerra JA. Biliary atresia: will blocking inflammation tame the disease? Annu Rev Med. 2011; 62:171–185. [PubMed: 21226614]
6. Asai A, Miethke A, Bezerra JA. Pathogenesis of biliary atresia: defining biology to understand clinical phenotypes. Nat Rev Gastroenterol Hepatol. 2015; 12:342–352. [PubMed: 26008129]
7. Feldman AG, Mack CL. Biliary Atresia: Clinical Lessons Learned. J Pediatr Gastroenterol Nutr. 2015; 61:167–175. [PubMed: 25658057]
8. Waisbourd-Zinman O, Koh H, Tsai S, Lavrut PM, Dang C, Zhao X, Pack M, Cave J, Hawes M, Koo KA, Porter JR, Wells RG. The toxin biliatresone causes mouse extrahepatic cholangiocyte damage and fibrosis through decreased glutathione and SOX17. Hepatology. 2016; 64:880–893. [PubMed: 27081925]
9. Serinet MO, Wildhaber BE, Broue P, Lachaux A, Sarles J, Jacquemin E, Gauthier F, Chardot C. Impact of age at Kasai operation on its results in late childhood and adolescence: a rational basis for biliary atresia screening. Pediatrics. 2009; 123:1280–1286. [PubMed: 19403492]
10. Sundaram SS, Mack CL, Feldman AG, Sokol RJ. Biliary atresia: Indications and timing of liver transplantation and optimization of pretransplant care. Liver Transpl. 2017; 23:96–109. [PubMed: 27650268]
11. Moyer V, Freese DK, Whitington PF, Olson AD, Brewer F, Colletti RB, Heyman MB. H North American Society for Pediatric Gastroenterology. Nutrition, Guideline for the evaluation of cholestatic jaundice in infants: recommendations of the North American Society for Pediatric Gastroenterology, Hepatology and Nutrition. J Pediatr Gastroenterol Nutr. 2004; 39:115–128. [PubMed: 15269615]
12. Jancelewicz T, Barmherzig R, Chung CT, Ling SC, Kamath BM, Ng VL, Amaral J, O'Connor C, Fecteau A, Langer JC. A screening algorithm for the efficient exclusion of biliary atresia in infants with cholestatic jaundice. J Pediatr Surg. 2015; 50:363–370. [PubMed: 25746690]

13. Song Z, Dong R, Fan Y, Zheng S. Identification of serum protein biomarkers in biliary atresia by mass spectrometry and enzyme-linked immunosorbent assay. J Pediatr Gastroenterol Nutr. 2012; 55:370–375. [PubMed: 22569524]
14. Zahm AM, Hand NJ, Boateng LA, Friedman JR. Circulating microRNA is a biomarker of biliary atresia. J Pediatr Gastroenterol Nutr. 2012; 55:366–369. [PubMed: 22732895]
15. Zhao D, Han L, He Z, Zhang J, Zhang Y. Identification of the plasma metabolomics as early diagnostic markers between biliary atresia and neonatal hepatitis syndrome. PLoS One. 2014; 9:e85694. [PubMed: 24416443]
16. Narayanaswamy B, Gonde C, Tredger JM, Hussain M, Vergani D, Davenport M. Serial circulating markers of inflammation in biliary atresia - Evolution of the postoperative inflammatory process. Hepatology. 2007; 46:180–187. [PubMed: 17596879]
17. Bessho K, Mourya R, Shivakumar P, Walters S, Magee JC, Rao M, Jegga AG, Bezerra JA. Gene expression signature for biliary atresia and a role for interleukin-8 in pathogenesis of experimental disease. Hepatology. 2014; 60:211–223. [PubMed: 24493287]
18. Gold L, Ayers D, Bertino J, Bock C, Bock A, Brody EN, Carter J, Dalby AB, Eaton BE, Fitzwater T, Flather D, Forbes A, Foreman T, Fowler C, Gawande B, Goss M, Gunn M, Gupta S, Halladay D, Heil J, Heilig J, Hicke B, Husar G, Janjic N, Jarvis T, Jennings S, Katilius E, Keeney TR, Kim N, Koch TH, Kraemer S, Kroiss L, Le N, Levine D, Lindsey W, Lollo B, Mayfield W, Mehan M, Mehler R, Nelson SK, Nelson M, Nieuwlandt D, Nikrad M, Ochsner U, Ostroff RM, Otis M, Parker T, Pietrasiewicz S, Resnicow DI, Rohloff J, Sanders G, Sattin S, Schneider D, Singer B, Stanton M, Sterkel A, Stewart A, Stratford S, Vaught JD, Vrkljan M, Walker JJ, Watrobka M, Waugh S, Weiss A, Wilcox SK, Wolfson A, Wolk SK, Zhang C, Zichi D. Aptamer-based multiplexed proteomic technology for biomarker discovery. PLoS One. 2010; 5:e15004. [PubMed: 21165148]
19. Tang KS, Huang LT, Huang YH, Lai CY, Wu CH, Wang SM, Hwang KP, Huang FC, Tiao MM. Gamma-glutamyl transferase in the diagnosis of biliary atresia. Acta Paediatr Taiwan. 2007; 48:196–200. [PubMed: 18265540]
20. Chen X, Dong R, Shen Z, Yan W, Zheng S. Value of Gamma-Glutamyl Transpeptidase for Diagnosis of Biliary Atresia by Correlation With Age. J Pediatr Gastroenterol Nutr. 2016; 63:370–373. [PubMed: 26963938]
21. Habibzadeh F, Yadollahie M. Number needed to misdiagnose: a measure of diagnostic test effectiveness. Epidemiology. 2013; 24:170.
22. Filippov S, Caras I, Murray R, Matrisian LM, Chapman HA Jr, Shapiro S, Weiss SJ. Matrilysin-dependent elastolysis by human macrophages. J Exp Med. 2003; 198:925–935. [PubMed: 12963695]
23. McGuire JK, Li Q, Parks WC. Matrilysin (matrix metalloproteinase-7) mediates E-cadherin ectodomain shedding in injured lung epithelium. Am J Pathol. 2003; 162:1831–1843. [PubMed: 12759241]
24. Li Q, Park PW, Wilson CL, Parks WC. Matrilysin shedding of syndecan-1 regulates chemokine mobilization and transepithelial efflux of neutrophils in acute lung injury. Cell. 2002; 111:635–646. [PubMed: 12464176]
25. Russo P, Magee JC, Boitnott J, Bove KE, Raghunathan T, Finegold M, Haas J, Jaffe R, Kim GE, Magid M, Melin-Aldana H, White F, Whitington PF, Sokol RJ. C. Biliary Atresia Research. Design and validation of the biliary atresia research consortium histologic assessment system for cholestasis in infancy. Clin Gastroenterol Hepatol. 2011; 9:357–362 e352. [PubMed: 21238606]
26. Parks WC, Wilson CL, Lopez-Boado YS. Matrix metalloproteinases as modulators of inflammation and innate immunity. Nature reviews Immunology. 2004; 4:617–629.
27. Riepenhoff-Talty M, Schaekel K, Clark HF, Mueller W, Uhnoo I, Rossi T, Fisher J, Ogra PL. Group A rotaviruses produce extrahepatic biliary obstruction in orally inoculated newborn mice. Pediatr Res. 1993; 33:394–399. [PubMed: 8386833]
28. Petersen C, Biermanns D, Kuske M, Schakel K, Meyer-Junghanel L, Mildenberger H. New aspects in a murine model for extrahepatic biliary atresia. J Pediatr Surg. 1997; 32:1190–1195. [PubMed: 9269968]

29. Shivakumar P, Campbell KM, Sabla GE, Miethke A, Tiao G, McNeal MM, Ward RL, Bezerra JA. Obstruction of extrahepatic bile ducts by lymphocytes is regulated by IFN-gamma in experimental biliary atresia. J Clin Invest. 2004; 114:322–329. [PubMed: 15286798]
30. Gottesman LE, Del Vecchio MT, Aronoff SC. Etiologies of conjugated hyperbilirubinemia in infancy: a systematic review of 1692 subjects. BMC Pediatr. 2015; 15:192. [PubMed: 26589959]
31. Peng X, Yang L, Liu H, Pang S, Chen Y, Fu J, Chen Y, Wen Z, Zhang R, Zhu B, Yu J, Invernizzi P. Identification of Circulating MicroRNAs in Biliary Atresia by Next-Generation Sequencing. J Pediatr Gastroenterol Nutr. 2016; 63:518–523. [PubMed: 26960174]
32. Dong R, Shen Z, Zheng C, Chen G, Zheng S. Serum microRNA microarray analysis identifies miR-4429 and miR-4689 are potential diagnostic biomarkers for biliary atresia. Sci Rep. 2016; 6:21084. [PubMed: 26879603]
33. Wang H, Malone JP, Gilmore PE, Davis AE, Magee JC, Townsend RR, Heuckeroth RO. Serum markers may distinguish biliary atresia from other forms of neonatal cholestasis. J Pediatr Gastroenterol Nutr. 2010; 50:411–416. [PubMed: 20216099]
34. Lee JY, Sullivan K, El Demellawy D, Nasr A. The value of preoperative liver biopsy in the diagnosis of extrahepatic biliary atresia: A systematic review and meta-analysis. J Pediatr Surg. 2016; 51:753–761. [PubMed: 26932252]
35. Leelawat K, Narong S, Wannaprasert J, Ratanashu-ek T. Prospective study of MMP7 serum levels in the diagnosis of cholangiocarcinoma. World J Gastroenterol. 2010; 16:4697–4703. [PubMed: 20872971]
36. Kuhlmann KF, van Till JW, Boermeester MA, de Reuver PR, Tzvetanova ID, Offerhaus GJ, Ten Kate FJ, Busch OR, van Gulik TM, Gouma DJ, Crawford HC. Evaluation of matrix metalloproteinase 7 in plasma and pancreatic juice as a biomarker for pancreatic cancer. Cancer Epidemiol Biomarkers Prev. 2007; 16:886–891. [PubMed: 17507610]
37. Morais A, Beltrao M, Sokhatska O, Costa D, Melo N, Mota P, Marques A, Delgado L. Serum metalloproteinases 1 and 7 in the diagnosis of idiopathic pulmonary fibrosis and other interstitial pneumonias. Respir Med. 2015; 109:1063–1068. [PubMed: 26174192]
38. Hung TM, Chang SC, Yu WH, Wang YW, Huang C, Lu SC, Lee PH, Chang MF. A novel nonsynonymous variant of matrix metalloproteinase-7 confers risk of liver cirrhosis. Hepatology. 2009; 50:1184–1193. [PubMed: 19676133]
39. Irvine KM, Wockner LF, Hoffmann I, Horsfall LU, Fagan KJ, Bijin V, Lee B, Clouston AD, Lampe G, Connolly JE, Powell EE. Multiplex Serum Protein Analysis Identifies Novel Biomarkers of Advanced Fibrosis in Patients with Chronic Liver Disease with the Potential to Improve Diagnostic Accuracy of Established Biomarkers. PLoS One. 2016; 11:e0167001. [PubMed: 27861569]
40. Huang CC, Chuang JH, Chou MH, Wu CL, Chen CM, Wang CC, Chen YS, Chen CL, Tai MH. Matrilysin (MMP-7) is a major matrix metalloproteinase upregulated in biliary atresia-associated liver fibrosis. Mod Pathol. 2005; 18:941–950. [PubMed: 15696117]
41. Kerola A, Lampela H, Lohi J, Heikkila P, Mutanen A, Hagstrom J, Tervahartiala T, Sorsa T, Haglund C, Jalanko H, Pakarinen MP. Increased MMP-7 expression in biliary epithelium and serum underpins native liver fibrosis after successful portoenterostomy in biliary atresia. J Pathol Clin Res. 2016; 2:187–198. [PubMed: 27499927]
42. Nissinen L, Kahari VM. Matrix metalloproteinases in inflammation. Biochimica et biophysica acta. 2014; 1840:2571–2580. [PubMed: 24631662]
43. Shivakumar P, Mizuochi T, Mourya R, Gutta S, Yang L, Luo Z, Bezerra JA. Preferential TNFalpha signaling via TNFR2 regulates epithelial injury and duct obstruction in experimental biliary atresia. JCI Insight. 2017; 2:e88747. [PubMed: 28289704]

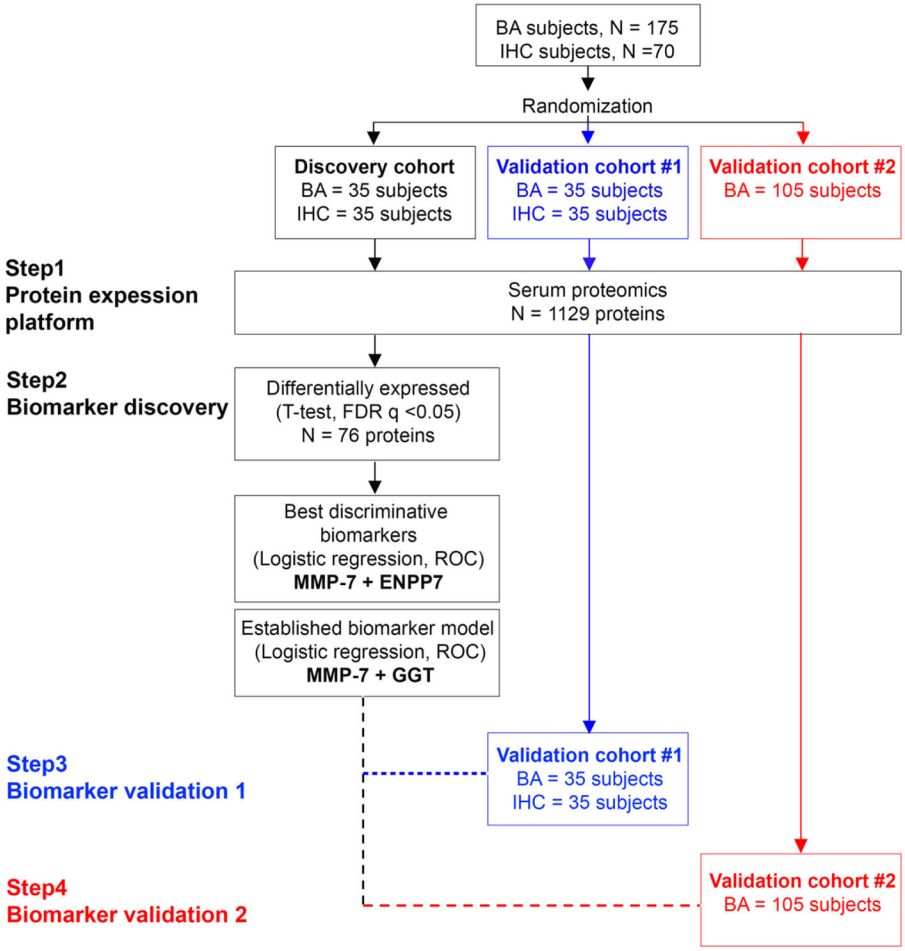

Fig. 1. Study design

A total of 175 biliary atresia (BA) subjects and 70 subjects with intrahepatic cholestasis (IHC) were randomized into the discovery cohort (BA=35, IHC=35), validation cohort #1 (BA=35, IHC=35) and validation cohort #2 (BA=105). Serum proteins were measured by high-throughput proteomic assay (SOMAscan®) separately for individual cohorts. FDR, false discovery rate; ROC, receiver operating characteristic.

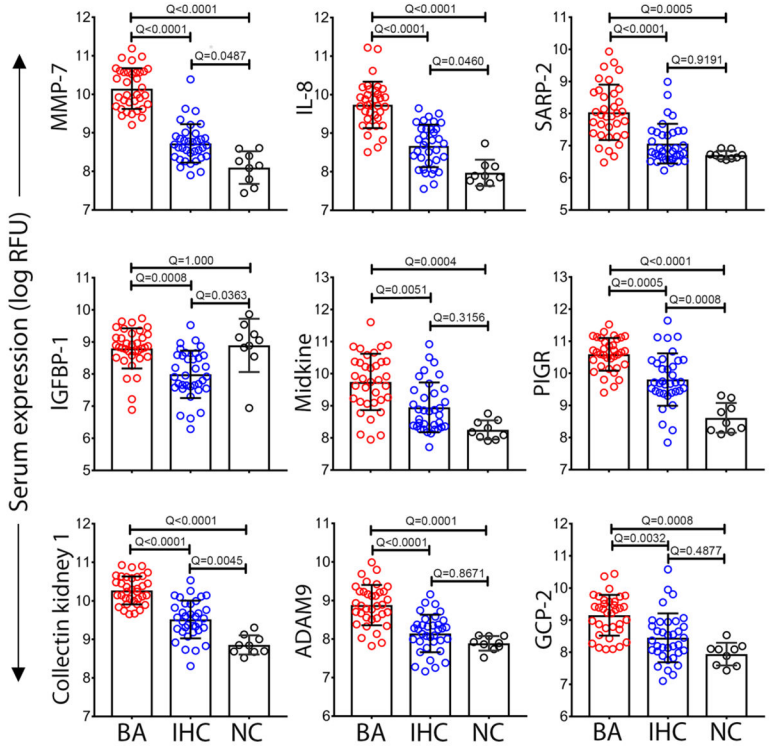

Fig. 2. Top 9 proteins differentially expressed between BA and IHC

Data from the discovery cohort categorized into biliary atresia (BA, N=35), intrahepatic cholestasis (IHC, N=35), and age-matched normal controls (NC, N=9). Dots represent the log of relative fluorescent unit (RFU) for individual serum proteins. Bars and whiskers represent median and interquartile range. Q-values from ANOVA with multiple hypothesis correction (Benjamini-Hochberg procedure).

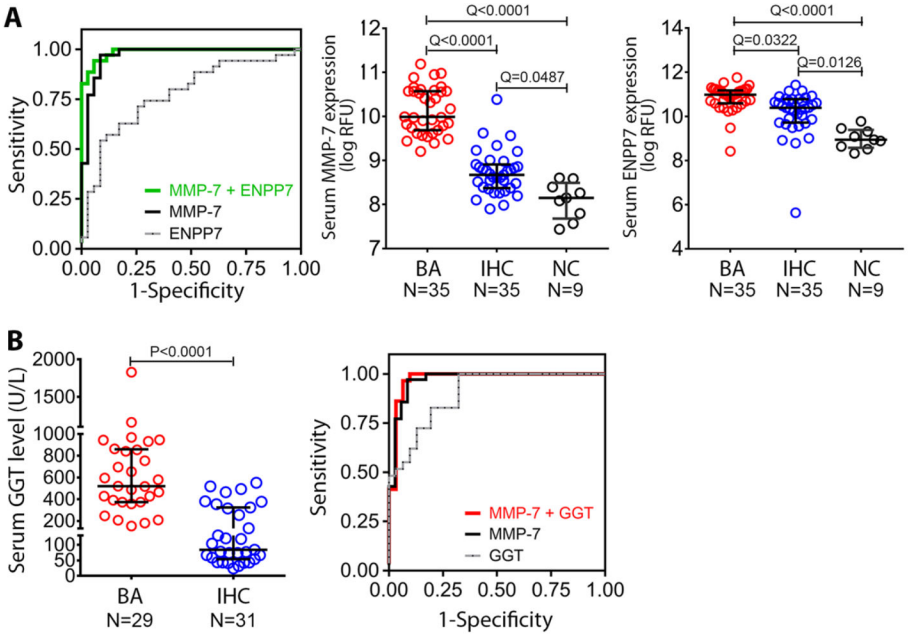

C

Prediction models	AUC (95%CI)	Sensitivity (%)	Specificity (%)	PPV (%)	NPV (%)	Accuracy (%)
MMP-7 +ENPP7	0.99 (0.97 to 1.00)	94	94	85	98	94
MMP-7	0.97 (0.93 to 1.00)	97	91	79	99	94
ENPP7	0.78 (0.66 to 0.89)	74	71	47	89	73
GGT	0.90 (0.83 to 0.97)	83	81	61	93	82
MMP-7 + GGT	0.98 (0.94 to 1.00)	97	94	85	99	95

Fig. 3. Predictive features of MMP-7, ENPP7 and GGT for biliary atresia

(A) ROC curves for serum MMP-7 and/or ENPP7 in distinguishing biliary atresia (BA) from intrahepatic cholestasis (IHC) in multivariable logistic regression analyses and dot plots of the proteins in the discovery cohort. Data are shown as log of relative fluorescent units (RFU); mid horizontal lines and whiskers represent median and interquartile range. (B) Serum GGT levels in subjects with BA and IHC; normal range is 5–59 U/L. The right panel shows ROC curves from MMP-7 and/or GGT. (C) Prediction models for MMP-7, ENPP7 and GGT. Sensitivity, specificity, positive and negative predictive values were calculated at selected optimal cut-off. Q values from ANOVA with multiple hypothesis correction (Benjamini-Hochberg procedure) for (A) and P-value from Mann Whitney test for (B). AUC, area under the ROC curve; NPV, negative predictive value; PPV, positive predictive value; ROC, receiver operating characteristic.

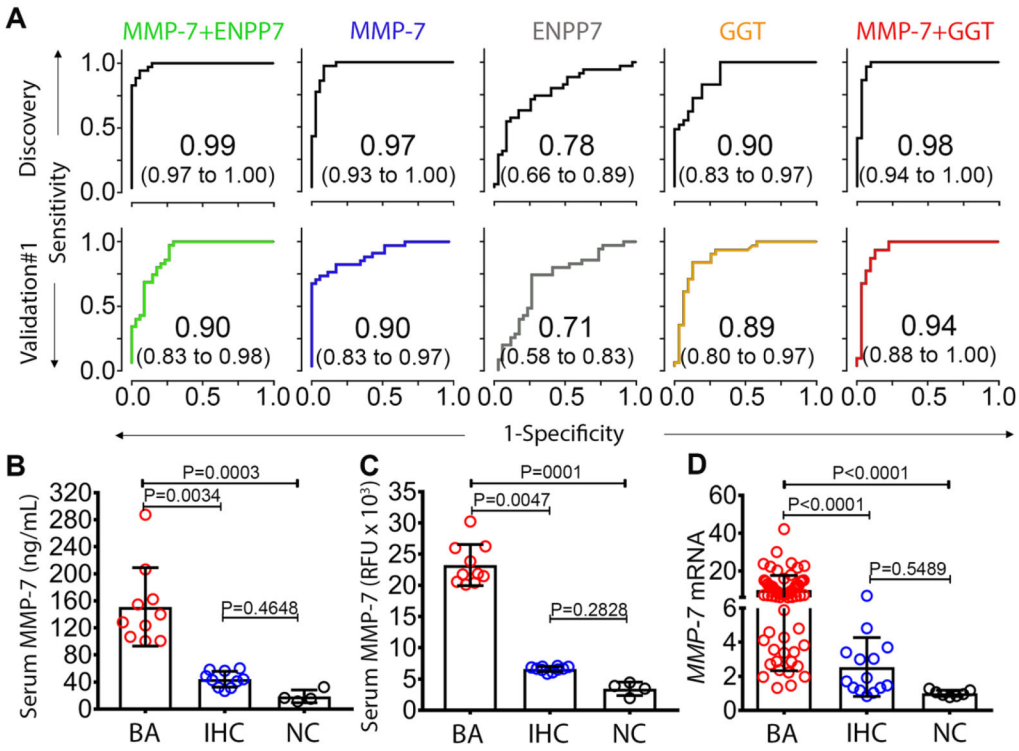

Fig. 4. MMP-7 biomarker validation and hepatic expression

(A) ROC curves in discovery and validation cohort #1 for MMP-7, ENPP7, and GGT. (B) Scatter plot of serum MMP-7 of randomly selected samples from biliary atresia (BA: N=10), intrahepatic cholestasis (IHC; N=10), and normal controls (NC; N=4) measured by antibody-based enzyme-linked immunosorbent assay compared with (C) the values measured by SOMAScan®. Data is presented as median and interquartile range. (D) Hepatic mRNA expression of *MMP-7* for BA (N=64), IHC (N=14), and NC (N=7). Expression levels are normalized to normal controls and are presented as fold change. P-values from Kruskal-Wallis test.

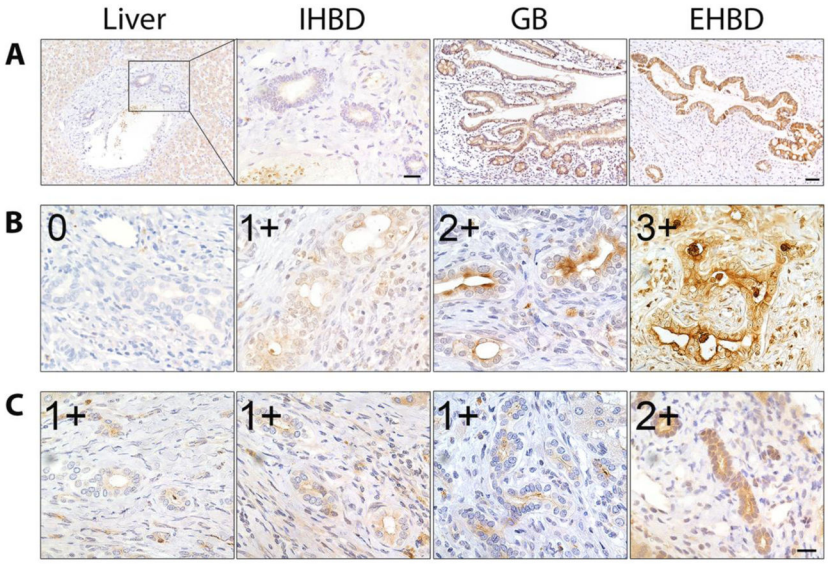

D

Intensity of signal in the intrahepatic bile ducts	Biliary atresia (N = 12)	A1AT deficiency (N=6)
0	16.67 %	-
1+	41.67 %	66.67 %
2+	33.33 %	33.33 %
3+	8.33 %	-

Fig. 5. MMP-7 expression in human liver, extrahepatic bile duct, and gallbladder

(A) Immunohistochemical staining of normal human liver shows minimal or no expression of MMP-7 in hepatocytes and intrahepatic bile ducts (IHBD), but intense expression in the biliary epithelium of gallbladder (GB) and extrahepatic bile duct (EHBD). Scale bars = 50 μm in liver, GB and EHBD and 20 μm in IHBD. (B) Increased expression of MMP-7 in the cytoplasm of intrahepatic biliary epithelium of biliary atresia subjects with variable intensity (0–3+). (C) Livers of patients with alpha-1 antitrypsin deficiency had lower MMP-7 expression in the intrahepatic bile ducts. Scale bar = 20 μm in (B) and (C). (D) Percentage of livers according to the intensity and extension of MMP-7 immunostaining in livers from patients with biliary atresia and alpha-1 antitrypsin deficiency.

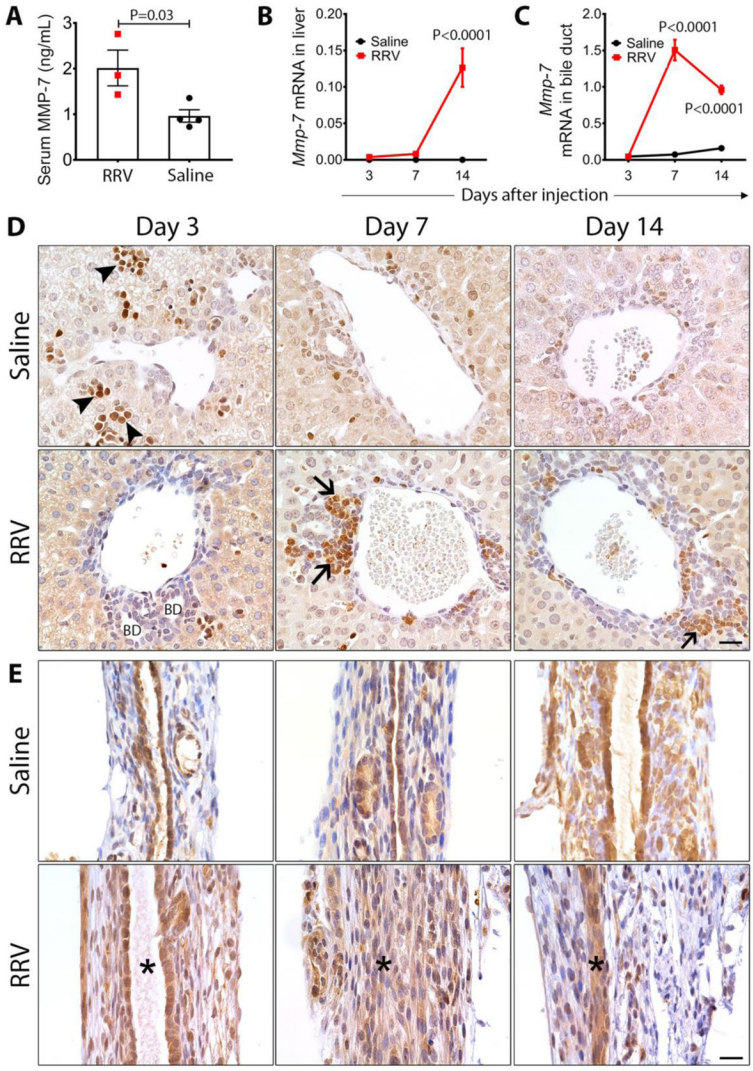

Fig. 6. Mmp-7 expression in experimental biliary atresia

(A) Serum Mmp-7 measured 7 days after rotavirus (RRV) or saline injection (N=3–4 per group). Mean±SEM, P-values from unpaired t-test. (B) *Mmp-7* mRNA expression in the livers and extrahepatic bile ducts (C) at 3, 7 and 14 days after RRV or saline injection (N= 3–4 per group and per time point). Values are normalized to *Gapdh* and are expressed as mean±SEM; P-values were between two groups at each time point (ANOVA). (D) Immunohistochemistry detects Mmp-7 in hematopoietic cells (arrowheads) predominantly at day 3, and inflammatory cells (arrows) infiltrating the portal tracts at day 7 and 14 after RRV injection. There was no staining of intrahepatic bile duct epithelium (BD). (E) Mmp-7 is detected in the duct epithelium in RRV and saline injected groups. At days 7 and 14 after injection, Mmp-7 is also detected in inflammatory cells and injured epithelium. Asterisks depict the duct lumen (or lack thereof); scale bars = 20 μm.

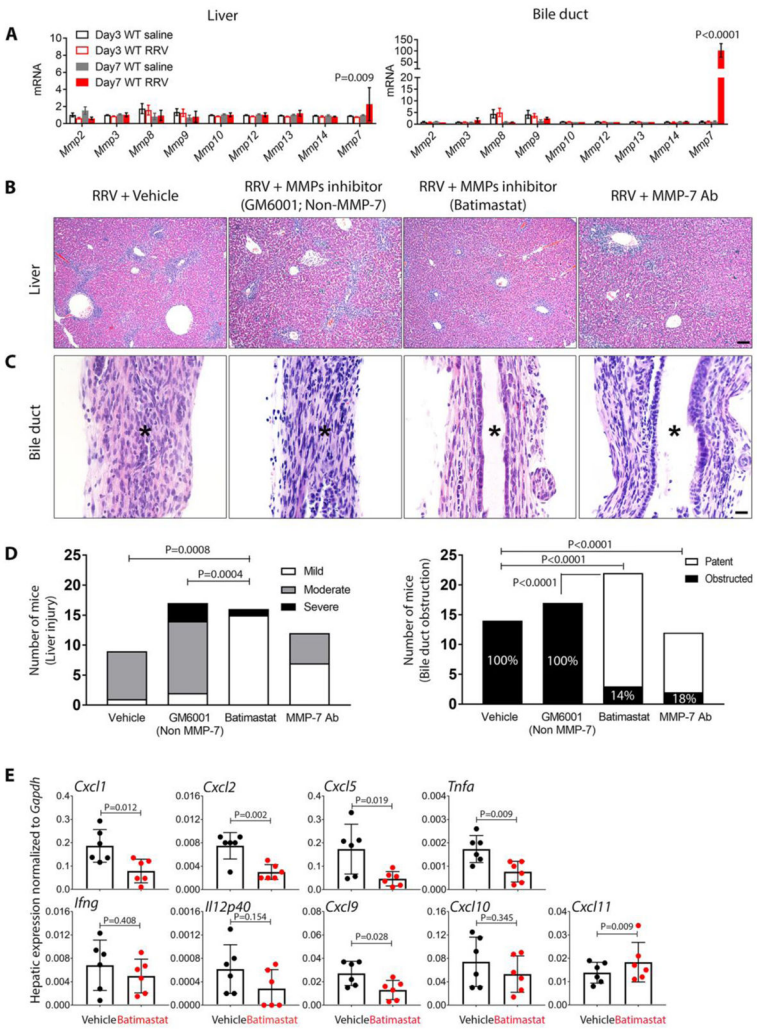

Fig. 7. Suppression of tissue injury, inflammation, and cytokine expression by Batimastat and MMP-7 antibody in experimental biliary atresia

Neonatal BALB/c mice were injected with RRV in the first day of life, then were injected with Batimastat (RRV + Batimastat; N=22) or GM6001 (Non-MMP-7, RRV + GM6001; N=17), anti-MMP-7 antibody (RRV + MMP-7 Ab; N=12) or vehicle in the control group (RRV + vehicle; N=14). (A) mRNA expression of tissue matrix metalloproteinases (*Mmps*) at 3 and 7 days after viral injection. (B) Representative liver sections showing variable degrees of portal inflammation and hepatic necrosis in different groups. (C) Representative sections of extrahepatic bile ducts in each group. Asterisks depict the duct lumen (or lack thereof); scale bars = 100 μm for (B) and 20 μm for (C). (D) Graphs depict the frequency of mice with liver injury, according to the degree of inflammation and hepatocellular necrosis, and frequency of mice with obstructed lumen. (E) Hepatic mRNA expression for cytokines/chemokines 12 days after RRV injection and treatment with Batimastat (inhibitor) or vehicle (as controls). P-values from ANOVA for (A), Chi-square for (D) and unpaired T-test for (E).

Table 1

Clinical and biochemical characteristics of subjects.

Variable	Discovery cohort			Validation cohort 1			Validation cohort 2	
	BA	IHC	*P**	BA	IHC	*P**	BA	*P***
Number of patients	35	35		35	34		105	
Age (days)	62±28	57±31	0.43	67±30	66± 35	0.24	72±28	0.07
Gender (F/M)	16/19	6/29		17/18	12/22		53/52	
AST (U/L)	268±381	246±208	0.61	211±135	270±258	0.59	233±192	0.65
ALT (U/L)	176±177	187±165	0.80	135±90	207±221	0.60	167±125	0.77
TB (mg/dL)	8.4±3.2	8.5±4.4	0.85	8.8±3.9	8.9±4.6	0.97	8.3±3.0	0.99
GGT (U/L)	619±361	179±169	<0.0001	744±519	241±305	<0.0001	842±629	0.11

Data are presented as the mean ± standard deviation. Mann-Whitney test was used.

* Comparison between biliary atresia (BA) and intrahepatic cholestasis (IHC).

** Comparison between BA in the discovery cohort and the validation cohort 2